Chemical Engineering Journal 101 (2004) 295–302

Chemical Engineering Journal

www.elsevier.com/locate/cej

Porous media simplified simulation of single- and two-phase flow heat transfer in micro-channel heat exchangers

U. Imke*

Forschungszentrum Karlsruhe, Institut für Reaktorsicherheit, P.O. Box 3640, 76021 Karlsruhe, Germany

Received 28 July 2003; accepted 13 October 2003

Abstract

A numerical tool to simulate micro-channel flow and heat transfer in compact heat exchangers is developed. The method is based on a forced convection porous body approach combined with conventional pipe flow closure correlations. The proposed technique aims to provide developers of micro-channel heat exchangers with a fast efficient tool to estimate the thermodynamic behaviour dependent on geometry and operation conditions. The program calculates outlet temperatures, pressure losses and vapour volume fractions, if boiling occurs. In addition the thermohydraulic conditions inside the heat exchanger can be determined. First results are compared to experiments with cross flow and counter flow heat exchangers for single-phase flow and with an electrical evaporator for boiling conditions.

Keywords: Micro-channel; Single-phase and two-phase flow; TwoPorFlow

1. Introduction

Micro-channel heat exchangers are beneficial in thermal and chemical process engineering applications when large heat transfer rates are needed and small sizes of the devices are of advantage [1]. To optimise the design of heat exchangers it is essential to have simulation tools describing the operational behaviour of the devices. Most of the actual procedures to simulate heat transfer in micro-channel heat exchangers ($D > 50\,\mu m$) are based on structure and fluid domain resolving calculations of single channels or groups of channels including fluid flow and conjugate heat transfer [1–5]. If possible the whole apparatus is mapped using commercial CFD codes with very high numerical effort. Such methods are limited by the number of simulated channels and the dimension of the apparatus including inlet and outlet. On the other hand, they are capable to handle complex geometries in detail. The situation becomes more complicated, if two-phase flow including phase change due to heat transfer is considered.

In this paper an approach based on empirical models is used to simulate micro-channel heat exchangers. This has several advantages compared to the use of more sophisticated geometry resolving up to date commercial CFD tools. The simplified tool models the main physical processes like heat conduction inside the solid structure, heat transfer to the fluid, pressure loss, momentum and heat exchange in two-phase flow by known empirical correlations. This makes the calculation more efficient and flexible. Characteristic data depending on different boundary and operating conditions can be produced using coarse meshing compared to usual CFD applications. Complicated and time-consuming grid generation is not necessary. Different channel geometries can be introduced simply by the hydraulic diameter combined with appropriate correlations for the Nusselt number. Switching from laminar to turbulent flow conditions is automatically taken into account by the constitutive correlations. For two-phase flow with boiling in micro-channel heat exchangers and void fractions up to one some simplified description of the physical problem as proposed in the following currently seems to be the only practical option.

For single-phase flow in micro-heat exchangers detailed CFD simulations and simplified simulations can complement each other. Commercial CFD tools have the advantage of the possibility to model nearly all kind of geometries in detail including housing and inlet–outlet regions and can also account for heat losses at arbitrary formed surfaces. They give detailed information about flow and heat flux inside the channels and in the structured material. Such tools can be used to compare their results with the conventional empirical pressure loss and Nusselt number correlations. With increasing computer power they have also the potential to produce characteristic parameter curves of the devices in future.

* Tel.: +49-7247-823802; fax: +49-7247-823718.
E-mail address: imke@irs.fzk.de (U. Imke).

1385-8947/$ – see front matter © 2004 Elsevier B.V. All rights reserved.
doi:10.1016/j.cej.2003.10.012

Nomenclature

C_{large}	large real number: 10^{12} (W/(m^3 K^2))
C_S	heat capacity of porous structure (J/(kg K))
D	hydraulic diameter (m)
e_L	internal energy of liquid (J/kg)
e_V	internal energy of vapour (J/kg)
F_I	friction at vapour–liquid interface (N/m^3)
F_{WL}	wall friction of liquid (N/m^3)
F_{WV}	wall friction of vapour (N/m^3)
$\vec{g}$	gravity (kg/(m s^2))
h	heat transfer coefficient (W/(m^2 K))
h_{bm}	modified Bromley coefficient (W/(m^2 K))
h_{dbm}	modified Dittus–Boelter coefficient (W/(m^2 K))
h_{mac}	Chen macro-convection coefficient (W/(m^2 K))
h_{mic}	Chen micro-convection coefficient (W/(m^2 K))
h_{SL}	saturation enthalpy of liquid (J/kg)
h_{SV}	saturation enthalpy of vapour (J/kg)
l	distance from channel entrance (m)
Nu	Nusselt number
Nu_{lam}	Laminar Nusselt number without entrance effect
P	pressure (Pa)
Pr	Prandtl number
Q_H	internal heat source in porous structure (W/m^3)
Q_I	heat exchange between phases (W/m^3)
Q_{IL}	liquid-interface heat exchange (W/m^3)
Q_{IV}	vapour-interface heat exchange (W/m^3)
Q_{WL}	heat exchange between structure and liquid (W/m^3)
Q_{WV}	heat exchange between structure and vapour (W/m^3)
Re	Reynolds number
t	time (s)
T_L	temperature of liquid (K)
T_S	temperature of porous structure (K)
T_{SAT}	saturation temperature (K)
T_V	temperature of vapour (K)
V_{MAX}	maximum velocity component in a mesh cell (m/s)
$\vec{V}_L$	velocity of liquid (m/s)
$\vec{V}_V$	velocity of vapour (m/s)
Δt	time step length (s)
Δx	mesh width (m)

Greek letters

α_L	volume fraction of liquid
α_V	volume fraction of vapour (void fraction)
Γ_I	rate of evaporation/condensation (kg/(m^3 s))
λ_S	thermal conductivity of porous structure (W/(m K))
μ_L	dynamic viscosity of liquid (Pa s)
ρ_L	density of liquid (kg/m^3)
ρ_S	density of structure (kg/m^3)
ρ_V	density of vapour (kg/m^3)

The method described in the present paper needs experimental validation of the models and closure laws. The essential integral results to be compared are the fluid temperature change and the pressure loss along the apparatus. In the case of two-phase flow void fraction or vapour quality could be compared in addition. Moreover, the simplified simulation provides information about the space distribution of temperature, pressure, velocity and liquid volume fraction inside the heat exchanger.

In the following sections the new computer code TwoPorFlow (two-phase porous flow) is presented. In the first part the method, the basic equations and the used closure laws are described. The second part shows the application of the code to different kinds of micro-channel heat exchangers.

2. Development of the code TwoPorFlow

2.1. Method

To realise a simplified efficient method taking into account the essential physical processes of flow and heat transfer in a micro-channel heat exchanger a porous media approach is used [6]. The code TwoPorFlow is developed to simulate single- and two-phase flow including heat transfer and phase change in multi-micro-channel devices. The two-fluid model [7] is taken to describe the flow of the liquid and gaseous fluids inside the one-dimensional channels. The solid structure is represented as a porous medium with its own temperature field. Wall friction, heat transfer between structure and fluid, and the momentum coupling between the fluid phases are modelled by conventional empirical correlations. Simplified equations of state and a boiling curve for water are implemented.

To solve the conservation equations for energy, mass and momentum in three-dimensional Cartesian coordinates a semi-implicit numerical procedure based on the implicit continuous Eulerian (ICE) method is used [7,8]. That method is particularly suitable for evaporation and condensation processes appearing in two-phase flow. The coupling with the solid structure heat conduction calculation is done in an explicit manner. Steady states are calculated by a transient approach.

2.2. Basic equations

TwoPorFlow is a two-phase code designed to describe a liquid and the appropriate vapour embedded in a regular or irregular structured porous body. The applications presented in Section 3 are characterised by unidirectional flows combined with three-dimensional heat conduction, but the code is generally able to calculate fluid convection in three dimensions. The meaning of the variables used in the following equations is given in the nomenclature.

The mass conservation equations for the two phases are:

$$\frac{\partial(\alpha_L \rho_L)}{\partial t} + \mathrm{div}(\alpha_L \rho_L \vec{V}_L) = -\Gamma_I \quad (1)$$

$$\frac{\partial(\alpha_V \rho_V)}{\partial t} + \mathrm{div}(\alpha_V \rho_V \vec{V}_V) = \Gamma_I \quad (2)$$

$$\alpha_L + \alpha_V = 1 \quad (3)$$

The source term Γ_I describes the rate of evaporation or condensation at the liquid–vapour interface.

The numerical solution procedure described later uses the momentum equations in non-conservative form:

$$\alpha_L \rho_L \frac{\partial \vec{V}_L}{\partial t} + \alpha_L \rho_L \vec{V}_L \,\mathrm{grad}(\vec{V}_L) + \alpha_L \,\mathrm{grad}(P) = -\vec{F}_{WL} + \vec{F}_I + \alpha_L \rho_L \vec{g} \quad (4)$$

$$\alpha_V \rho_V \frac{\partial \vec{V}_V}{\partial t} + \alpha_V \rho_V \vec{V}_V \,\mathrm{grad}(\vec{V}_V) + \alpha_V \,\mathrm{grad}(P) = -\vec{F}_{WV} - \vec{F}_I + \alpha_V \rho_V \vec{g} \quad (5)$$

Momentum transfer by phase change is not taken into account. The gravity term is not important for the flow in micro-channel heat exchangers and is set to zero in the calculations. The friction between fluid and wall is given by $\vec{F}_{WL}$ and $\vec{F}_{WV}$, whereas the coupling at the liquid–vapour interface is provided by $\vec{F}_I$.

For energy conservation the internal energy is used as the main variable:

$$\frac{\partial(\alpha_L \rho_L e_L)}{\partial t} + \mathrm{div}(\alpha_L \rho_L e_L \vec{V}_L) + P\,\mathrm{div}(\alpha_L \vec{V}_L) + P\frac{\partial \alpha_L}{\partial t} = Q_{WL} - Q_I \quad (6)$$

$$\frac{\partial(\alpha_V \rho_V e_V)}{\partial t} + \mathrm{div}(\alpha_V \rho_V e_V \vec{V}_V) + P\,\mathrm{div}(\alpha_V \vec{V}_V) + P\frac{\partial \alpha_V}{\partial t} = Q_{WV} + Q_I \quad (7)$$

where Q_{WL} and Q_{WV} are the heat transfer terms between porous structure and liquid and vapour, respectively. Q_I describes the heat flux at the liquid–vapour interface coupled to evaporation and condensation processes. Γ_I and Q_I are linked by the vapour-interface and liquid-interface heat fluxes:

$$Q_{IV} + \Gamma_I h_{SV} = Q_I \quad (8)$$

$$Q_{IL} - \Gamma_I h_{SL} = -Q_I \quad (9)$$

The two equations can be combined to calculate the mass transfer:

$$\Gamma_I = -\left(\frac{Q_{IV} + Q_{IL}}{h_{SV} - h_{SL}}\right) \quad (10)$$

The heating of the fluid from wall friction is neglected. It plays a role for large velocities in pure gas micro-channel flows and will be implemented later in TwoPorFlow.

The heat conduction equation in the porous body is given by

$$\rho_S C_S \frac{\partial T_S}{\partial t} = \mathrm{div}(\lambda_S \,\mathrm{grad}(T_S)) - Q_{WL} - Q_{WV} + Q_H \quad (11)$$

where Q_H is a volumetric heat source inside the structure, which can be used to simulate electrical heating for instance.

In the case of a single-phase flow simulation the number of equations is reduced to account for the corresponding phase only, and the phase coupling terms are set to zero.

2.3. Closure correlations

There is an intense discussion in the literature whether the conventional constitutive equations for pressure loss and heat transfer of pipe flow can be used for micro-channels. Some authors find different behaviour for the transition from laminar to turbulent flow and deviations for the Nusselt number. A critical review is found in Refs. [9,10]. In Ref. [11] it is concluded that the conventional Navier–Stokes and energy equations can accurately predict the heat transfer and pressure loss characteristics of micro-channel heat sinks with ($231\,\mu m \times 713\,\mu m$) rectangular channels. For boiling heat transfer Kandlikar [12] gives a review about the most important effects like nucleation, flow patterns, pressure loss and heat transfer. It is indicated that as a first-order estimate heat transfer may be predicted using the flow boiling correlations developed for large diameter tubes.

In the examples presented in this paper the conventional equations for heat transfer and friction are used without modifications, but if necessary special micro-channel correlations will be implemented for future studies. Most of the well known correlations are given with reference to the literature, whereas some specialities of TwoPorFlow are explained explicitly. The wall friction for single-phase flow is modelled by simple laminar and turbulent pressure loss coefficients for one-dimensional channel flow as given in Ref. [13]. In the turbulent regime the Blasius correlation is used. The transition from laminar to turbulent flow is realised by using a transition spline function between the Reynolds number of 2000 and 2600. For two-phase flow the Lockhart-Martinelli multiplier is apportioned between the friction terms of the vapour and liquid momentum equation applying the method described by Kelly and Kazimi [14].

For the momentum exchange between the phases three different models are available: equal velocities, a drift flux model and a two-fluid simplified coupling correlation given by Kelly and Kazimi [14], which is used in the present calculations and given here:

$$\vec{F}_I = \frac{1.01 - \hat{\alpha}_V}{\hat{\alpha}_V D}\left[\frac{1.01 - \hat{\alpha}_V}{\hat{\alpha}_V D}\mu_L + \frac{\rho_V |\vec{V}_V - \vec{V}_L|}{2}\right] \times (\vec{V}_V - \vec{V}_L) \quad (12)$$

$$\hat{\alpha}_V = \max(\alpha_V, 0.1) \quad (13)$$

The first term accounts for the drag of vapour bubbles moving through the liquid. The second term represents a form loss resulting from the motion of two continuous streams describing the annular flow regime. The above correlation substitutes a more complicated momentum coupling flow map, which is not available for micro-channel flow in detailed form. Virtual mass effects are not included, because only steady-state results are of interest here.

In a first version of TwoPorFlow the mass and energy exchange terms related to evaporation and condensation are set to describe a homogeneous mixture of vapour and liquid at saturation temperature. This condition can be reached by setting

$$Q_{\mathrm{IL}} = -C_{\mathrm{large}}(T_{\mathrm{SAT}} - T_{\mathrm{L}})^2 \tag{14}$$

for super-heated water and

$$Q_{\mathrm{IV}} = C_{\mathrm{large}}(T_{\mathrm{SAT}} - T_{\mathrm{V}})^2 \tag{15}$$

for sub-cooled vapour, where C_{large} is a large real number (10^{12} W/(m^3 K^2)) to drive the temperature of vapour and liquid close to the saturation temperature. However, in general the code is prepared to simulate thermal non-equilibrium, too. In this case appropriate equations have to be defined for Q_{IV} and Q_{IL}.

For non-boiling cases the heat transfer between porous structure walls and the fluids is given by standard Nusselt number correlations used for conventional channel flow. Actually the formulas from the VDI-Wärmeatlas [13] are used. A correlation for irregular non-channel-type structures is provided, too [15]. The transition from laminar to turbulent heat transfer is made continuously differentiable by using a transition spline function between the Reynolds number of 2000 and 2600 as used for the wall friction.

For convective boiling of the saturated liquid the well known heat transfer correlation of Chen is used in the form given by Kolev [16]. The minimum film boiling temperature is computed by equations given by Groenveld and Stewart [17]. The film boiling correlations are taken from the two-phase flow code THERMIT [14]. The combination of all these correlation defines the boiling curve for the liquid, which is qualified for water only. A short summary of the used heat transfer correlations is given in Table 1.

The simplified equations of state and property functions for water are taken from THERMIT [14]. For other fluids under single-phase flow conditions polynomial coefficients can be given as input to build appropriate state and property functions.

2.4. Numerical solution

The numerical solution of the basic equations combined with the closure laws is based on a finite-volume method with a staggered grid configuration in three-dimensional Cartesian coordinates. All scalar variables are cell-centred. The velocity components are located on cell faces. All convective terms are calculated with a standard first-order donor cell scheme. Time integration is first-order semi-implicit, whereas the momentum convective terms are treated explicitly. The non-conservative momentum equations are written as finite-difference equations. They are rearranged in a way that the new time step velocities are rewritten as a linear function of the local and adjacent cell implicit pressures. The set of conservative continuity and energy equations is cell volume integrated in consideration of the volume and area porosities given by input. The velocity components in the cell boundary flux terms are eliminated by the linear pressure functions derived from the momentum equations. Now a set of equations is defined for the void fraction, α_{V}, the internal energies, e_{L} and e_{V}, and the pressure, P, at the end of the time step. These equations are solved by a Newton–Raphson method using the temperatures instead of the internal energies as main variables. All non-linear implicitly taken values are replaced by a first-order development with respect to the main variables. The derivatives of the closure laws for mass and heat transfer have to be calculated, if they are treated implicitly.

The resulting system of equations to be solved for each Newton iteration couples the change per time step of void fraction, of liquid and vapour temperature and pressure in a cell with the change of pressure in the six adjacent cells. After inversion of a 4×4 matrix at each cell a Poisson problem for the pressure changes remains to be solved. A direct solver based on a Cholesky-type method is used. From the pressure changes the changes of the other main variables are calculated. The Newton method converges dependent on a user-controlled pressure criterion. Using the linear pressure-dependent functions for velocity components the new velocities can be calculated from the new pressure field at the end of the time step. The described procedure is an extension of the implicit continuous Eulerian (ICE) method developed for single-phase flow [8]. It is specially suited for

Table 1
Heat transfer coefficients used in TwoPorFlow for the present applications

Flow regime	Source	Type of correlation
Laminar forced convection	VDI-Wärmeatlas [13]	$Nu = \sqrt[3]{Nu_{\mathrm{lam}}^3 + 1.61^3 Re\,Pr\,D/l}$
Turbulent forced convection ($P_{\mathrm{r}} \leq 1.5$)	VDI-Wärmeatlas [13]	$Nu = 0.0214(Re^{0.8} - 100.0)Pr^{0.4}[1.0 + (D/l)^{2/3}]$
Turbulent forced convection ($P_{\mathrm{r}} > 1.5$)	VDI-Wärmeatlas [13]	$Nu = 0.012(Re^{0.87} - 280.0)Pr^{0.4}[1.0 + (D/l)^{2/3}]$
Convective nucleate boiling	Kolev [16]	$h = h_{\mathrm{mac}} + h_{\mathrm{mic}}$
Convective film boiling	Kelly and Kazimi [14]	$h = h_{\mathrm{dbm}} + h_{\mathrm{bm}}$

flows with phase change, because source terms (mass and energy exchange) can be handled implicitly. A more detailed description and the advantages of that method are reported in Ref. [7].

The heat conduction equation of the porous structure is solved with a finite-volume method, too, but all terms are treated fully explicit.

Stationary solutions are found by performing a transient calculation starting with appropriate initial and boundary conditions and stopping the simulation if steady state is reached for the main state variables. The time step is limited by the Courant condition using the convective velocities and the thermal behaviour of the porous structure given by the expressions:

$$\Delta t \leq \min_{\text{cells,directions}} \left(\frac{\Delta x}{V_{\text{MAX}}} \right) \tag{16}$$

$$\Delta t \leq \min_{\text{cells,directions}} \left(0.5 \frac{\rho_S c_S}{\lambda_S} (\Delta x)^2 \right) \tag{17}$$

In addition the user can control the time step by giving upper limits for the change of the main variables per time step.

3. Applications

3.1. Cross flow heat exchanger

For single-phase water flow in a 1 cm^3 cubic cross flow micro-channel heat exchanger integral results with TwoPorFlow have been obtained and compared with measurements [1,4]. The heat exchanger is made of 50 stainless steel foils with 34 micro-channels per foil. The rectangular channels with a cross-section of 200 μm × 100 μm have a length of 14 mm. The width of the fins and the bottom is 100 μm. Each foil has two neighbouring foils on top and bottom rotated by 90°. Only 10 mm of the channel length has direct contact to the crossing neighbour (Fig. 1). Neglecting heat losses at the device surfaces one cross flow module containing two foils is used in the simulation. This module is substituted by a porous body with a volume porosity of 0.33 subdivided into a mesh of 2 × 48 × 48 cells including small inlet and outlet flow regions. Blocking walls which set the mass flow rate between the numerical cells to zero are used to force the flow directions and to separate the different passages. Inside the inlet region the fluid flow is distributed automatically to the different channels dependent on the local pressure loss. The outlet region provides the system with a homogeneous outlet pressure given by the experimental settings. The mass flow rates of the initially cold water (8 °C) in one passage and the warm water (95 °C) in the other passage are the same. For the channel inlet and outlet pressure loss coefficients an estimated value of 1.0 is assumed. The course of water temperature change and pressure loss during the flow through the device depending on the mass flow rate can be calculated nearly in accordance with the measured curves (Figs. 2–4) without using any further special fitting parameters. The results are generated by a continuous quasi-steady-state run changing the inlet water flow rates smoothly in time. Using an "IBM pSeries630 POWER4" AIX workstation the CPU time to get the continuous curves is about 1 h. Deviations in the temperature behaviour can be caused by using a constant Nusselt number of 3.4 for laminar flow, although the heat flow is not uniformly distributed around the channels and the temperature along the channel structure is not constant. Pressure loss is more difficult to calculate, because small deviations from the nominal geometry strongly influence the result. Moreover, inlet and outlet pressure losses can be estimated, only. Around a flow rate of 350 kg/h the flow in the warm passage becomes turbulent, which can be seen clearly in the pressure loss curve changing

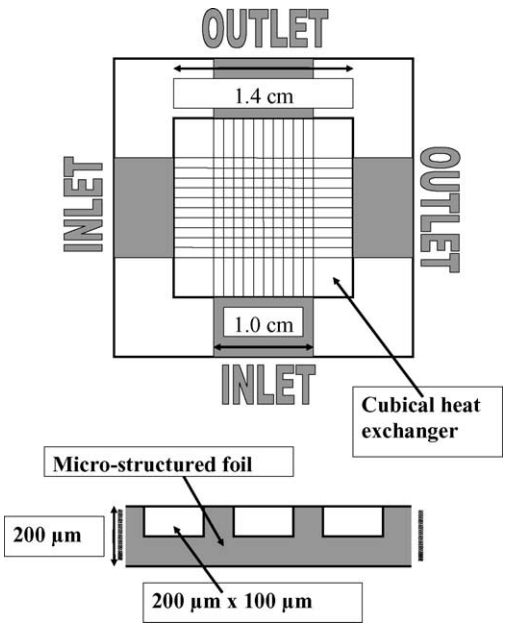

Fig. 1. Principle of micro-channel cross flow heat exchanger.

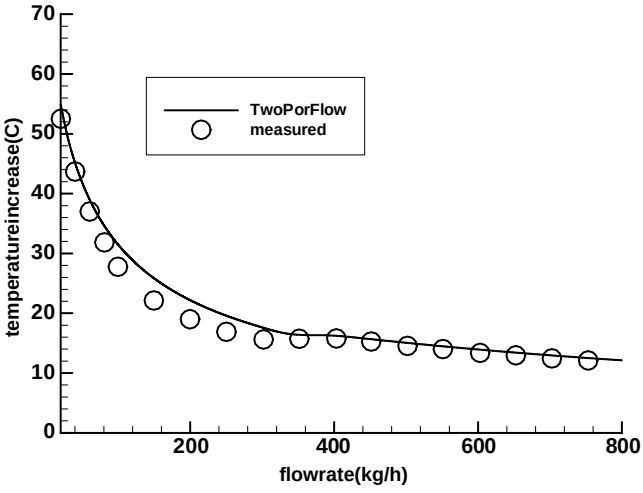

Fig. 2. Temperature increase of cold inlet water leaving the cross flow heat exchanger dependent on the flow rate.

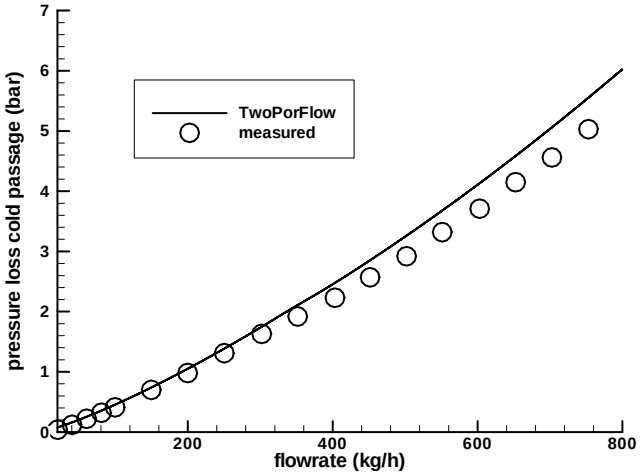

Fig. 3. Pressure loss in passage entered by cold water in the cross flow heat exchanger.

its slope (Fig. 4). The good agreement of experimental result and simulation shows that the transition from laminar to turbulent flow occurs in the present case at a Reynolds number of about 2300 as in conventional pipe flow.

3.2. Counter flow heat exchanger

The counter flow heat exchanger is made of one double-sided structured stainless steel foil with 20 (200 μm × 200 μm) channels on both sides with a length of 18.5 cm. The width of the fins is 100 μm and the total thickness of the foil is 600 μm (Fig. 5). The foil is enclosed by a massive stainless steel housing including inlet and outlet, which is not considered in the simulation. Two adjacent channels with opposite flow directions lying one on top of the other are used as representative region of the heat exchanger. That region is substituted by a porous body with a porosity of 0.44 subdivided into a mesh of 1 × 2 × 37

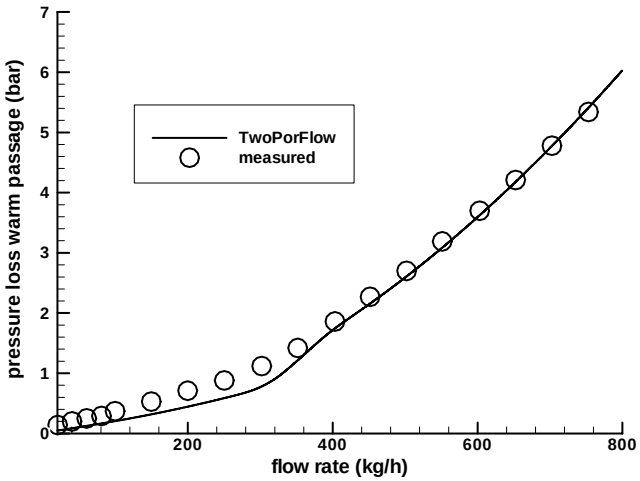

Fig. 4. Pressure loss in passage entered by warm water in the cross flow heat exchanger.

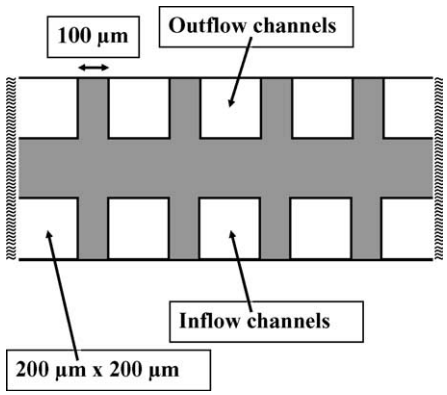

Fig. 5. Principle of counter flow heat exchanger.

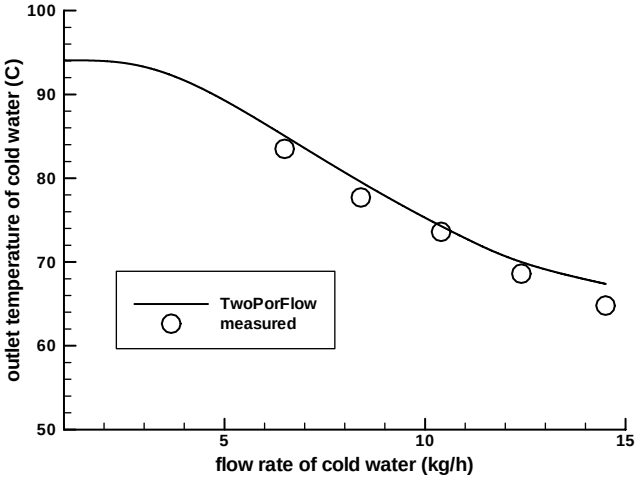

Fig. 6. Counter flow outlet temperature for the cold inlet water.

cells. The warm inlet passage (94 °C) has a constant feed of 20 kg/h, whereas the water flow rate at the cold inlet is varied. The calculation needs a CPU time of 20 min. Figs. 6 and 7 show the temperatures at the outlet dependent on that flow condition. The temperature predictions given by the

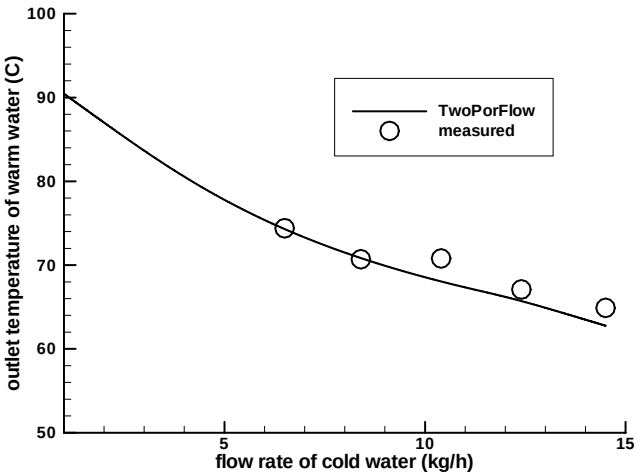

Fig. 7. Counter flow outlet temperature for the warm inlet water.

TwoPorFlow code compare quite well with the experimental data, but the pressure loss is overestimated in this case. For the warm passage with constant flow rate a pressure loss of 9 bar is calculated compared to a measurement of 7 bar only. The pressure loss is sensitive to small cross-section area deviations and the channel surface roughness which is not taken into account in the actual code version. Besides, the pressure is measured in the inlet and outlet regions outside the micro-channels. The effect of entrance flow at a group of sharp-edged channels is simulated by pressure loss coefficient estimation.

3.3. Electrically heated evaporator

Between two stainless steel plates a number of micro-structured stainless steel foils and spacer blocks are arranged in alternating order. Cartridge resistor heaters are inserted into holes of the spacer blocks. For the present example six foils each with 103 (200 μm × 100 μm × 54 mm) channels are heated with a maximum power of 900 W and cooled by a water flow rate of 4.4 kg/h with an inlet temperature of 18 °C (Fig. 8). The arrangement of the channels inside the foils is the same as for the cross flow heat exchanger (Fig. 1). During the experiment the power and the pressure boundary conditions at the outlet are changed. The flow rate is held constant. More details about this kind of micro-evaporators are documented in Ref. [1].

The two-phase flow simulation with TwoPorFlow is done in a simplified one-dimensional model. A homogeneous power distribution is assumed and one representative channel is simulated with 27 axial mesh cells. Under the above-mentioned conditions (change of system pressure) a quasi-steady-state run cannot be performed to generate a continuous result. For each parameter point new initial conditions (power and pressure) are used to get a stable steady-state solution after running a transient. The main difficulty in two-phase flow simulation in such small channels is the occurrence of flow and pressure oscillations at the outlet under boiling conditions. They can be caused by physical and numerical reasons. In the present case a stable solution can be found, because no dry-out of the channels occurs and the inlet mass flow is fixed. Simulation of boiling needs more CPU time than single-phase flow calculations. For the present results about 20 min are taken by TwoPorFlow.

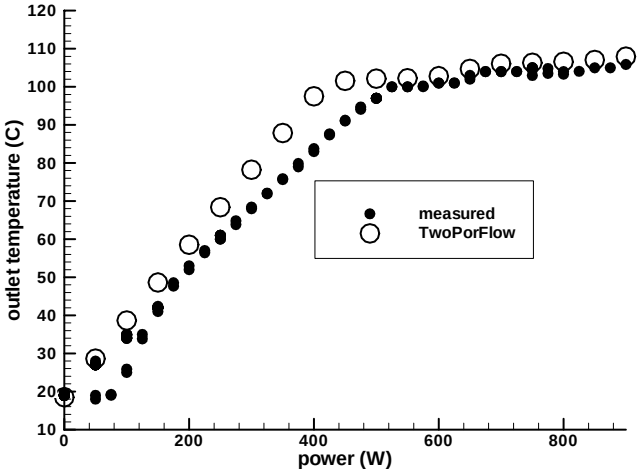

Fig. 9. Outlet temperature of the electrically heated evaporator.

Fig. 9 shows the outlet temperature dependent on the electric power inserted into the device. After onset of boiling the curve becomes flat because the saturation temperature is dependent on pressure only and no overheating of vapour occurs. Generally the temperature is a little bit overestimated due to heat losses in the experimental setup not considered in the simulation. Due to the fact that the heat source is not directly located inside the microstructure, heat losses play a more important role than in the devices described in previous sections. For the inlet pressure shown in Fig. 10 the general tendency is reproduced, but for single-phase liquid flow the pressure loss is underestimated.

The distribution of velocities and void fraction along the heated micro-channels in the boiling region is plotted in

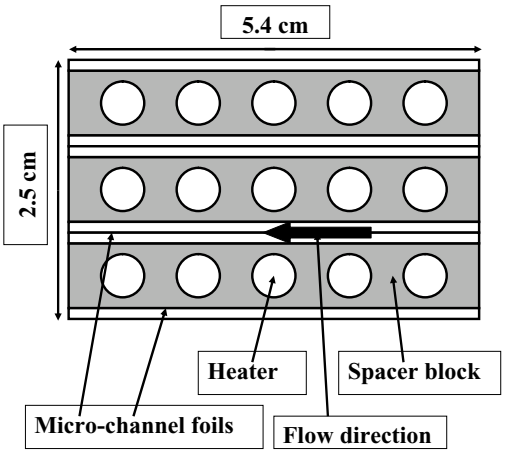

Fig. 8. Principle of electrically heated micro-channel evaporator.

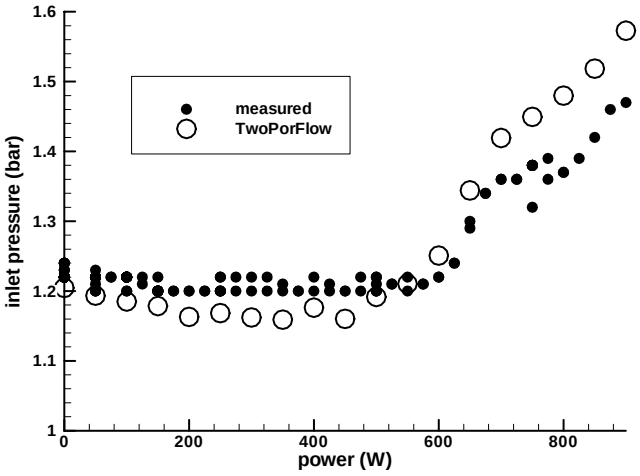

Fig. 10. Inlet pressure of the electrically heated evaporator.

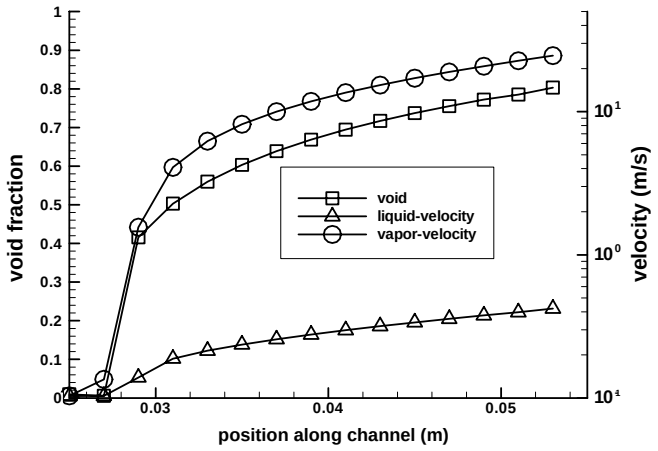

Fig. 11. Velocities and vapour volume fractions along the micro-channels inside the electrical evaporator operated at 900 W.

Fig. 11 for the maximum power used in the actual experiment. The void fraction curve is characterised by a sharp increase near the inlet. Consistent with this behaviour the vapour velocity becomes much larger resulting in stronger pressure losses.

4. Conclusions

The numerical simulation tool TwoPorFlow is developed to calculate efficiently estimations of the behaviour of different micro-channel heat exchangers operating in a single- or two-phase flow mode. Pressure losses, temperatures and boiling conditions can be predicted using a porous media forced convection approach combined with empirical conventional closure correlations known from normal-sized channel flow. The code is open for implementation of special micro-channel correlations, if necessary. The actual program was applied to a single-phase flow cross heat exchanger and a counter flow heat exchanger, both operated with water. First two-phase flow simplified one-dimensional simulations were made for an electrically heated water evaporator. The results for heat transfer (temperatures) agree well with the experimental findings. Larger deviations are found for the pressure loss, which is much more sensitive to the manufacturing accuracy of the channel geometry or deposits at the channel walls, for instance. The code can be used to produce characteristic curves for the devices under different operating conditions. Even the simplified simulation can give valuable information about the conditions inside the used devices.

Acknowledgements

The author wishes to acknowledge the support of the personnel of the “Institut für Mikroverfahrenstechnik” of the “Forschungszentrum Karlsruhe” who provide the experimental data for the different micro-channel heat exchangers.

References

[1] K. Schubert, J. Brandner, M. Fichtner, G. Linder, U. Schygulla, A. Wenka, Microstructure devices for applications in thermal and chemical process engineering, Microscale Thermophys. Eng. 5 (2001) 17–39.
[2] W. Qu, I. Mudawar, Analysis of three-dimensional heat transfer in micro-channel heat sinks, Int. J. Heat Mass Transfer 45 (2002) 3973–3985.
[3] K.C. Toh, X.Y. Chen, J.C. Chai, Numerical computation of fluid flow and heat transfer in microchannels, Int. J. Heat Mass Transfer 45 (2002) 5133–5141.
[4] A. Wenka, M. Fichtner, K. Schubert, Investigation of the thermal properties of a micro heat exchanger by three-dimensional fluid dynamics simulation, in: Proceedings of the Fourth International Conference on Microreaction Technology (IMRET 4), AIChE Spring Nat. Meeting, Atlanta, GA, 5–9 March 2000; Topical Conference Proceedings, New York, NY, 2000, pp. 256–263.
[5] A. Wenka, J. Brandner, K. Schubert, A computer-based simulation of the thermal processes in an electrically powered micro heat exchanger, in: Proceedings of the Sixth International Conference on Microreaction Technology (IMRET 6), New Orleans, LA, 10–14 March 2002.
[6] H.Y. Zhang, X.Y. Huang, Heat transfer studies of a porous heat sink characterized by straight circular ducts, Int. J. Heat Mass Transfer 44 (2001) 1593–1603.
[7] H.B. Stewart, B.B. Wendroff, Review—two-phase flow: models and methods, J. Comput. Phys. 56 (1984) 363–409.
[8] F.H. Harlow, A. Amsden, A numerical fluid dynamics calculation method for all flow speeds, J. Comput. Phys. 8 (1971) 197–213.
[9] N. Obot, Towards a better understanding of friction and heat/mass transfer in microchannels—a literature review, in: G.P. Celata, et al. (Eds.), Proceedings of the Heat Transfer and Transport Phenomena in Microscale, Banff, Canada, 15–20 October 2000, Begell House Publication, New York, 2000, pp. 72–79.
[10] H. Herwig, O. Hausner, Technical note, critical view on “new results in micro-fluid mechanics”: an example, Int. J. Heat Mass Transfer 46 (2003) 935–937.
[11] W. Qu, I. Mudawar, Experimental and numerical study of pressure drop and heat transfer in a single-phase micro-channel heat sink, Int. J. Heat Mass Transfer 45 (2002) 2549–2565.
[12] S.G. Kandlikar, Fundamental issues related to flow boiling in minichannels and microchannels, Exp. Therm. Fluid Sci. 26 (2002) 389–407.
[13] VDI-Wärmeatlas: recherchieren, berechnen, konstruieren Berechnungsblätter für den Wärmeübergang/Verein Deutscher Ingenieure VDI-Gesellschaft Verfahrenstechnik und Chemieingenieurwesen (GVC), Springer, 9. Auflage, 2002.
[14] J.E. Kelly, M.S. Kazimi, Development of the two fluid multi-dimensional code THERMIT for LWR analysis, American Institute of Chemical Engineers Symposium Series No. 199, vol. 76, 1980, pp. 149–161.
[15] S.J. Kim, S.P. Jang, Effects of the Darcy number, the Prandtl number, and the Reynolds number on local thermal non-equilibrium, Int. J. Heat Mass Transfer 45 (2002) 3885–3896.
[16] N.I. Kolev, Multiphase flow dynamics 2, in: Mechanical and Thermal Interactions, Springer, Berlin, 2002, p. 499 ff.
[17] D.C. Groenveld, J.C. Stewart, The minimum film boiling temperature for water during film boiling collapse, in: Proceedings of the Seventh International Heat Transfer Conference, vol. 5, Munich, 1982.